VTT Technical Research Centre of Finland

Fast Fracture Analyses for Boiling Water Reactor Pressure Vessel and Its Internals

Cronvall, Otso

Published in:
Baltica XI

Published: 01/01/2019

Document Version
Publisher's final version

Fast Fracture Analyses for Boiling Water Reactor Pressure Vessel and Its Internals

Otso Cronvall

VTT Technical Research Centre of Finland Ltd
Espoo, Finland

Abstract

This study concerns fast fracture analyses to a Finnish Boiling Water Reactor Pressure Vessel (BWR RPV) and one significant internal component for the most severe anticipated loading event while also taking into account the long-term operation (LTO) period. The considered components are the RPV and the core shroud. The reference cracks and procedures according to the ASME Section XI [1] Appendix G are applied in the analyses. The sizes of the corresponding critical cracks are computed as well. For the ferritic RPV wall the analysis takes the decrease of the material fracture toughness due to irradiation embrittlement into account. The core shroud wall is of stainless steel and therefore is not susceptible to irradiation embrittlement. It is concluded that the criteria of ASME Section XI Appendix G are fulfilled. The additional margins against fast fracture are large. It is further concluded that the critical crack sizes are so large that even much smaller cracks would be found during the yearly RPV inspections.

1. Introduction

Both the Finnish regulator STUK and the Finnish government have recently granted TVO the permission to continue the operational life of the OL1/OL2 units from 40 to 60 years. Of these two units OL1 has already entered the LTO period. The RPV and its internals have to fulfil their pressure tightness and functional requirements until the end-of-life (EOL). Therefore, it is necessary to perform degradation propagation analyses considering all relevant degradation mechanisms. These analyses have obviously been already performed to OL1 and OL2. Significant examples of these analyses include the fast fracture analyses for the RPV the core shroud. These analyses together with their results are summarized in this study. As a phenomenon or definition fast fracture is something from between brittle and ductile fracture, being nearer to the former one.

The considered analysis cases are reference cracks according to the ASME Section XI [1] Appendix G as well as critical cracks. The analyses are performed for the following locations:

- RPV wall, and
- core shroud wall.

The fast fracture analyses are performed for the most severe anticipated loading event. Where applicable, irradiation embrittlement is taken into account. Figure 1-1 shows the components considered in the analyses.

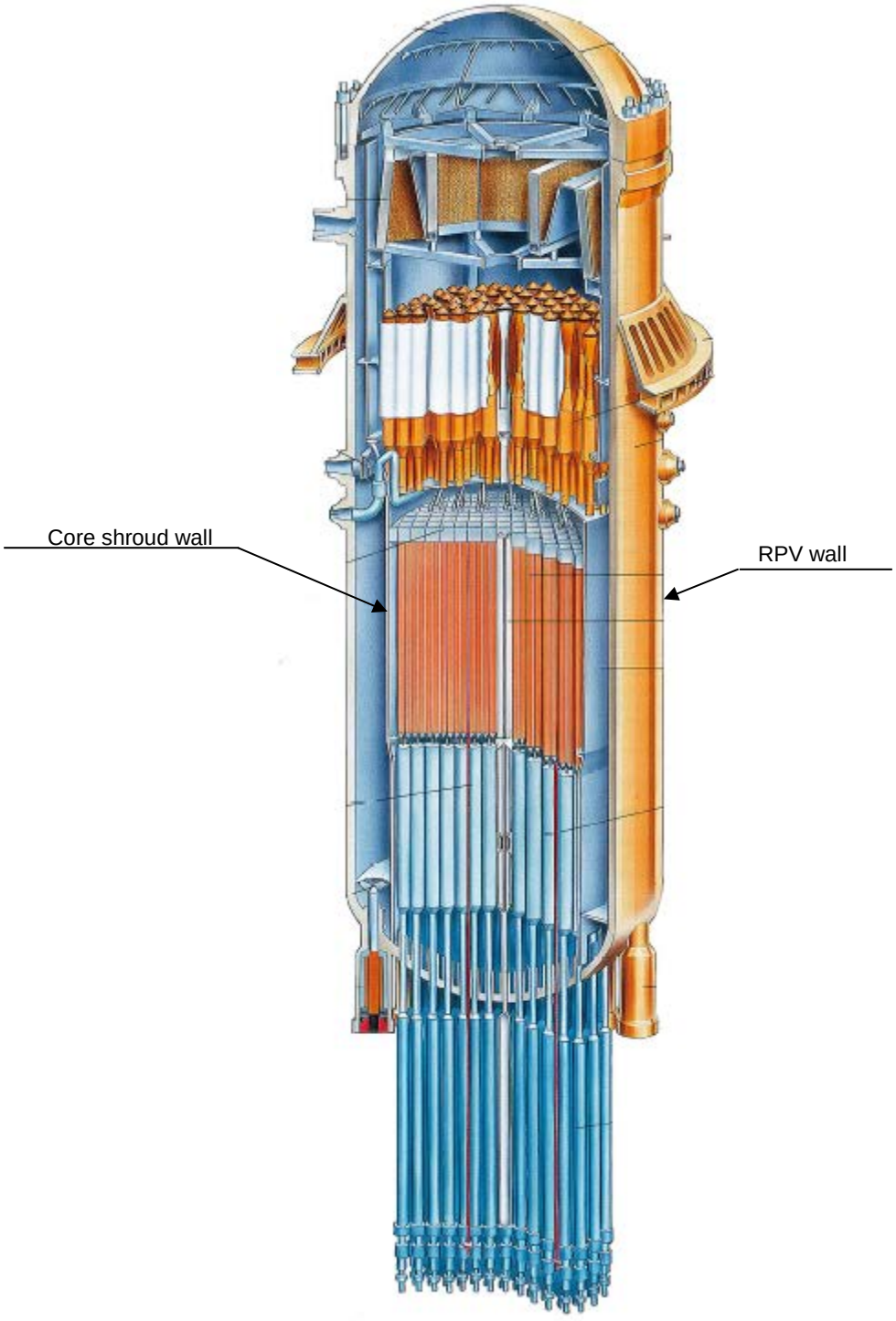

Figure 1-1. The considered RPV and the locations considered in the analyses [2].

2. Procedure used in the fast fracture analyses

Fast fracture means rupture that is not preceded by significant overall deformation. The ASME Section XI [1] recognizes brittle fracture and ductile fracture but not fast fracture. To overcome this the fast fracture procedure described in ref. [3] is applied where necessary.

According to ref. [3] the fast fracture is defined as:

1. Ductile crack propagation. This is weakly temperature dependent and requires a high amount of plastic deformation ahead of the crack front.
2. Brittle or semi-brittle fracture. This depends strongly on temperature and the size of the crack front.

For ferritic steels the fracture toughness transition curves are computed as follows:

- Get the applicable transition temperature for the 41 J absorbed energy T_{41J} [°C] temperature data from measurements done to surveillance specimens.
- Get the applicable fluence data from as recent analysis as possible.
- Using T_{41J} as input data, compute fracture toughness reference temperature T_0 [°C] with ASTM E 1921 [4] procedure. For convenience this procedure is also repeated below, see equation (2-1).
- Using T_0 as input data, compute the reference nil-ductility temperature RT_{T0} [°C] according to Paragraph G-2110 of ref. [1].
- Using RT_{T0} as input data, compute the fracture toughness K_{Ic} [MPa√m] values according to Paragraph G-2110 of ref. [1].

$$T_0 = T_{41J} + C \tag{2-1}$$

where C = -14 °C for this analysis.

The analysis procedure for fast fracture is as follows:

1. Take the K_{Ic} value after irradiation embrittlement.
2. Determine the stress intensity factor K_I [MPa√m] values at the crack tip and crack edge points. In this study this is done by using analysis code VTTBESIM, see refs. [5], [6], and analytical equations, see refs. [7], [8].
3. Determination of the occurrence of the fast fracture, in this case using the procedure in Appendix G of ref. [1]. For convenience, this procedure is also repeated below, see equation (2-2).

$$2K_{Im} + K_{It} < K_{Ic} \tag{2-2}$$

where: K_{Im} [MPa√m] is K_I due to membrane tension and K_{It} [MPa√m] is K_I due to thermal loading.

Equation (2-2) shall be satisfied for Levels A and B Service conditions for all crack postulates. From equation (2-2) it can be seen that a safety factor of 2 is applied on the stress intensity resulting from the non-self-equilibrating loads.

3. Input data

The input data needed in the analyses of this study is summarized in the following. This consists of the following parts:

- Geometry and crack postulates.
- Material properties.
- Load Cases and Loading Combinations.

3.1 Geometry and crack postulates

The section geometry and material regions of the RPV wall are presented in Figure 3-1. A vertical section of the core shroud is presented in Figure 3-2.

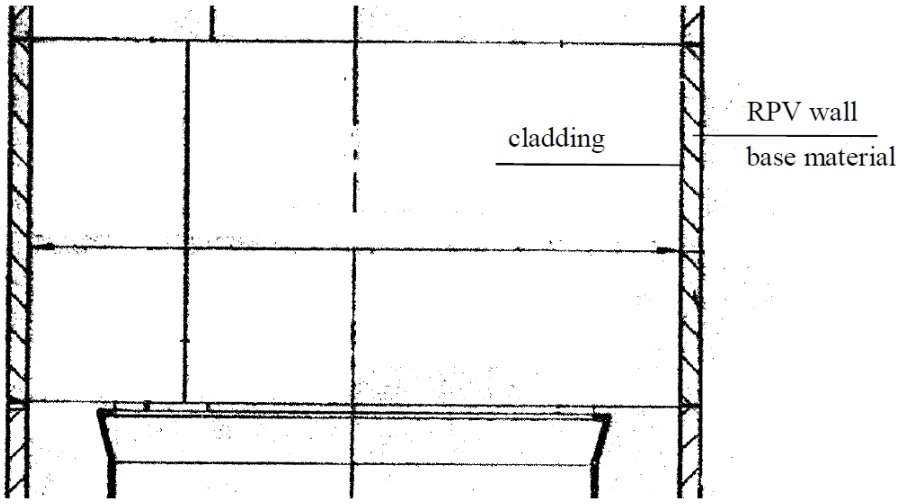

Figure 3-1. The RPV wall section geometry and material regions [9].

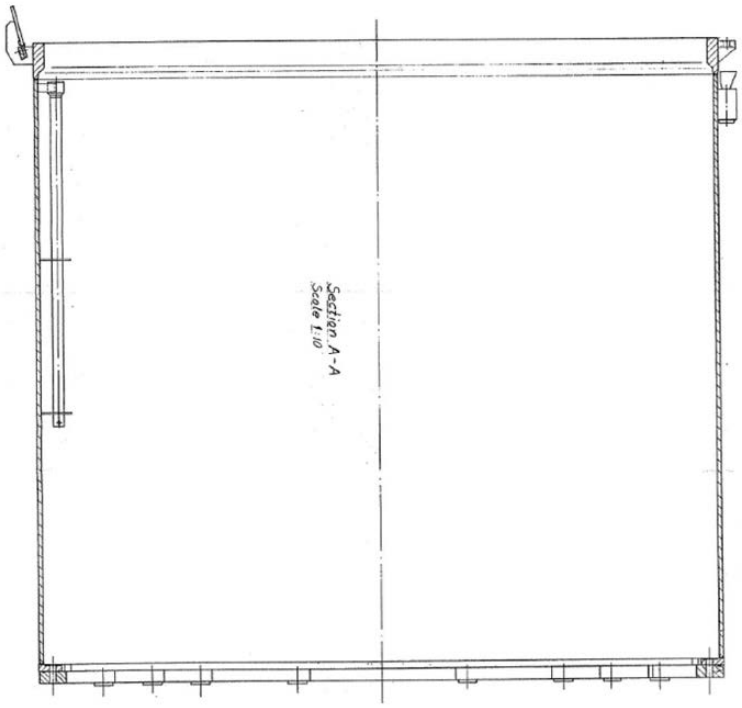

Figure 3-2. Vertical section of the core shroud [10].

The RPV wall reference crack => According to Appendix G of ref. [1] the requirements are:

- It is a sharp defect breaking to inner surface.
- It is orientated:
  - axially for plates, forgings, and axial welds,
  - circumferentially for circumferential welds.
- For a wall thickness > 102 mm:
  - It has a depth of ¼ times the wall thickness,
  - It has a length of 1½ times the wall thickness.

Thus, the following reference cracks are considered for the RPV wall:

- An axially orientated crack with depth x length a×l = 34.8×208.5 mm.
- A circumferentially orientated crack with a×l = 34.8×208.5 mm.

For an illustration of the axially orientated RPV wall crack postulate, see Figure 3-3.

The core shroud wall reference crack => the requirements are:

- According to Appendix G of ref. [1]: "For wall thickness < 102 mm a 25 mm deep defect is conservatively postulated. Smaller defect sizes may be used on an individual case basis if a smaller size of maximum postulated defect can be ensured."
- As here the wall thickness is approximately 25 mm, a 25 mm deep crack is too conservative. According to Appendix A of ref. [11] => if wall thickness t ≤ 40 mm, a = ½×t and l×6 x a.

Thus, the following reference cracks are considered for the core shroud wall:

- An axially orientated outer surface breaking crack with a×l = 12.5×75.0 mm.
- A circumferentially orientated outer surface breaking crack with a×l = 12.5×75.0 mm.

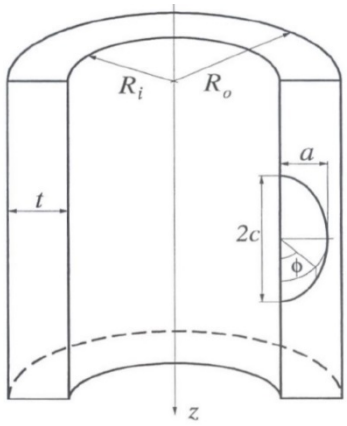

Figure 3-3. Illustration of the axially orientated RPV wall crack postulate.

In preliminary analyses for the RPV wall and the core shroud wall it was discovered that only through wall cracks are large enough to be critical cracks, i.e. having the maximum K_I value over the crack front reaching K_{Ic}.

3.2 Material properties

The materials of the considered components are presented in Table 3-1 below. The cladding at the inside of the RPV was included in the analyses. The strength properties of the involved materials are presented Table 3-2 below. Therein, T is temperature, Sy is yield strength and Su is ultimate strength, respectively.

Table 3-1. The material types of the considered components.

Component	Material region	Material type
RPV	wall	ferritic steels
	cladding	austenitic stainless steel
Core shroud	wall	austenitic stainless steel

Table 3-2. The strength properties of the involved materials of the considered components. The sources to this data are refs. [12], [13].

T	RPV wall		RPV cladding		Core shroud	
	Sy	Su	Sy	Su	Sy	Su
[°C]	[MPa]	[MPa]	[MPa]	[MPa]	[MPa]	[MPa]
20	345	552	172	483	205	475
300	292	552	108	393	152	420

The computed fracture toughness properties for the analysed components are presented in the following.

For the RPV wall the fracture toughness transition curves are computed according to the procedure described in Section 2. The following results are given after 60 years in operation:

- $T_0 \approx$ -40 °C,
- $RT_{T0} \approx$ -18 °C.

The resulting K_{Ic} transition curves after 0, 40 and 60 years in operation are shown in Figure 3-4.

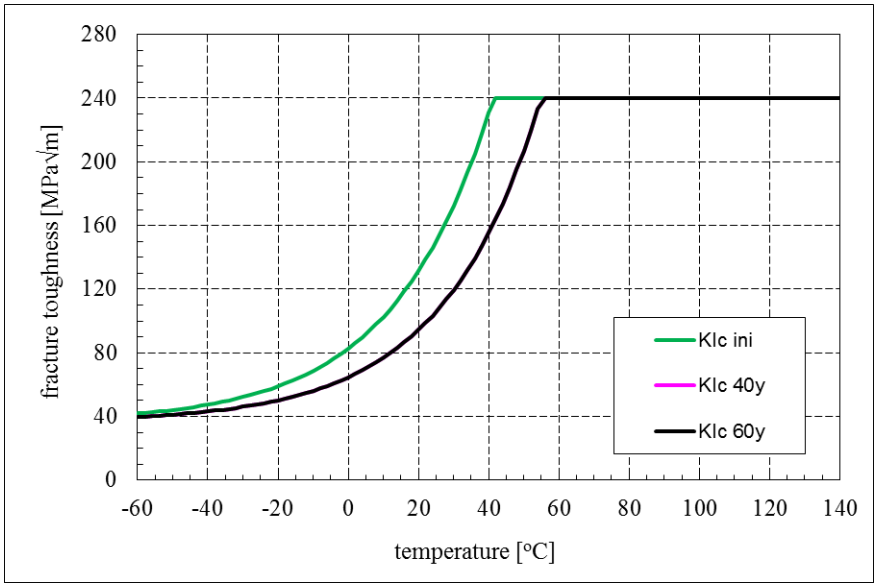

Figure 3-4. The resulting K_{Ic} transition curves after 0, 40 and 60 years in operation. In the legend "ini" is at the start of operation, "40y" is after 40 years of operation, and "60y" is after 60 years of operation.

As the base material of the core shroud wall is not susceptible to irradiation embrittlement, the beginning-of-life (BOL) values are used. For the fracture toughness, handbook recommendations for austenitic stainless steels are applied [14], see Table 3-3 below. This data was available only for one temperature.

Table 3-3. Fracture toughness data for austenitic stainless steels [14].

T	J_{Ic}	K_{Ic}
[°C]	[kJ/m^2]	[MPa√m]
288	620	350

3.3 Load Cases and Loading Combinations

According to the Appendix G of ref. [1], Levels A and B Service conditions shall be considered. For Levels A and B the influence of global dynamic load cases is insignificant. Therefore, the 100 % normal operation is the only relevant stationary load case. This load case is presented in Table 3-4 below.

Table 3-4. 100 % normal operation load case for Finnish BWR units [15]. Here p is pressure and NA is not applicable.

Component	***T***	***p***
	[°C]	[MPa]
RPV wall	286	7.0
Core shroud wall	NA	NA

The influence of the force and moment loads from the piping was studied. It was discovered that the effect is insignificant.

The considered transient load case is the automatic depressurization (ADS). During ADS both pressure and temperature decrease rapidly from their operational values to those of one atmosphere and room temperature. ADS has remained as an additional design load case, as this far it has not occurred in Finnish BWR units. The ADS is described in more detail below.

As for the RPV, only its inner surface is loaded:

- The loading events occur in the RPV downcomer. This takes place in the gap between the RPW wall and core shroud wall and corresponds to a water flow downwards, see Figure 1-1.
- The load data in question is presented in Figure 3-5.
- Both the temperature and pressure loads from the inside are taken into account in the RPV stress analyses.

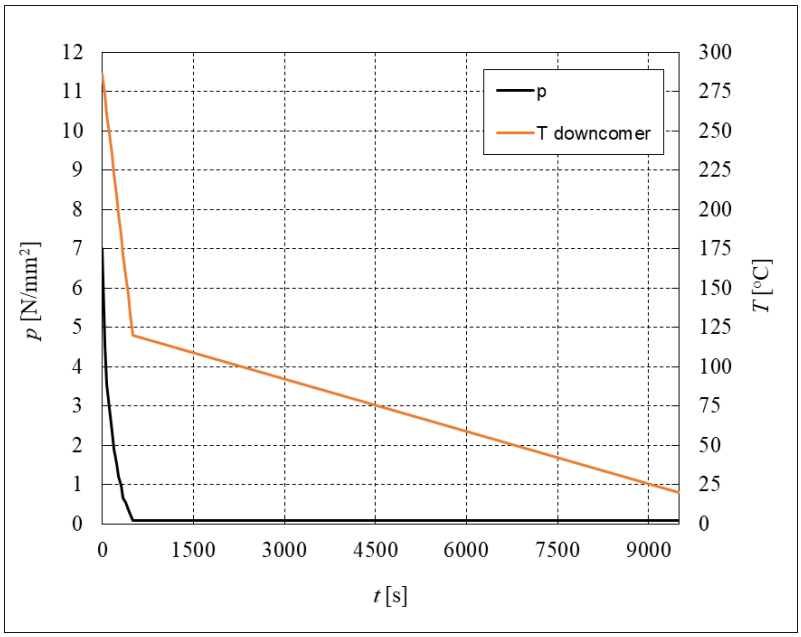

Figure 3-5. Thermal and pressure transient ADS in the RPV downcomer [16].

- As for the core shroud, both its outer and inner surfaces of are loaded:
- For the outer surface it is the RPV downcomer, see explanation above and Figure 1-1.
- The temperature load at the inside of the shroud changes at a slightly slower rate than that at the outside, see Figure 3-6.

- According to earlier analysis results the pressure fluctuation at the outside and inside of the core shroud is equal. Therefore, there are no pressure loads over the core shroud wall during the ADS.
- Only the temperature loads from both the inside and outside are taken into account in the stress analyses.

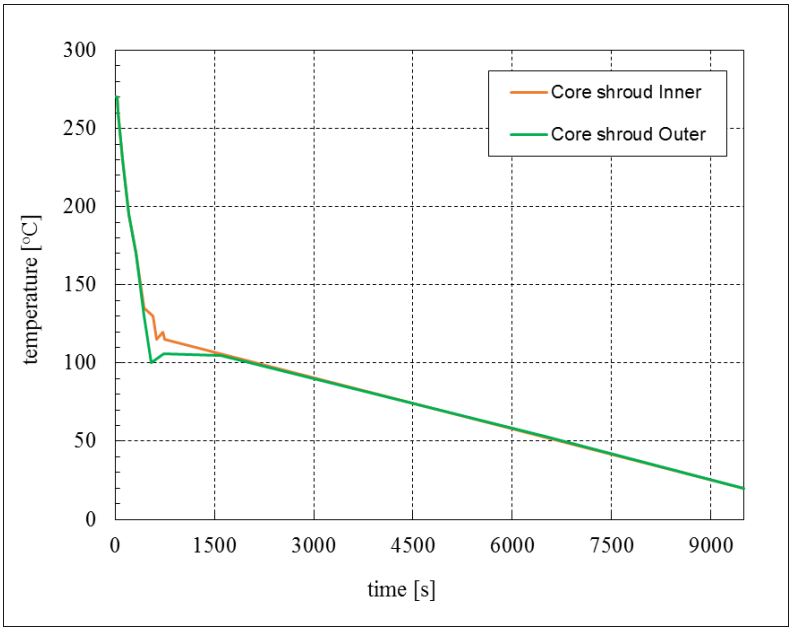

Figure 3-6. Temperatures caused by transient ADS near inner and outer surfaces of the core shroud [16].

4. Stress analyses

The stress analyses performed to the considered components are described in the following.

4.1 RPW wall

The stresses induced by the temperature and pressure loads were computed with the finite difference method based analysis code DIFF [17]. The considered load cases are 100 % normal operation followed by ADS. The cladding is included in the analyses.

The residual stresses between the cladding and the adjoining base material are not taken into account. This is because:

- The crack postulates are so large that only a very small portion of their fronts belong to the cladding region.
- The maximum K_I value is reached at the crack tip for which the effect of the cladding region is negligible.

The stress free temperature for both the base material and the cladding was taken as 286 °C, which is the 100 % operational temperature inside the RPV. For justification of this, see e.g. ref. [18]. The stress results for a number of through-wall locations are presented in Figures 4-1 and 4-2. In the legends, the numbers mean radial distance in mm from the inner surface which in turn is 0.0.

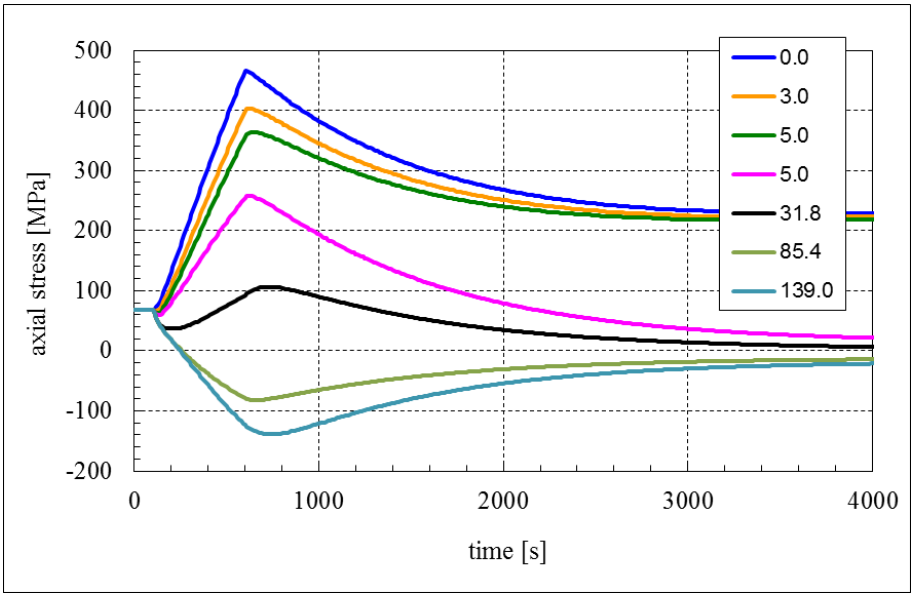

Figure 4-1. ADS transient => RPV wall axial stress time history (0 is at inner surface).

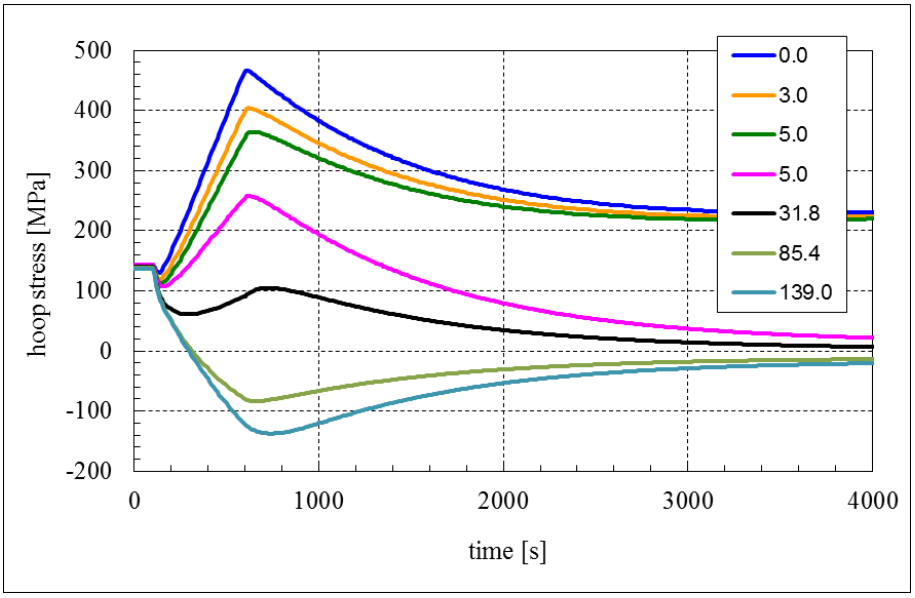

Figure 4-2. ADS transient => RPV wall hoop stress time history (0 is at inner surface).

4.2 Core shroud wall

The stresses induced by the temperature load were determined with the DIFF code [17]. The considered load cases are 100 % normal operation followed by ADS. The temperature load is applied both to the outer and inner surfaces. For a number of locations through the wall the results are presented in Figures 4-3 and 4-4. In the legends the numbers mean radial distance in mm from the inner surface which in turn is 0.0.

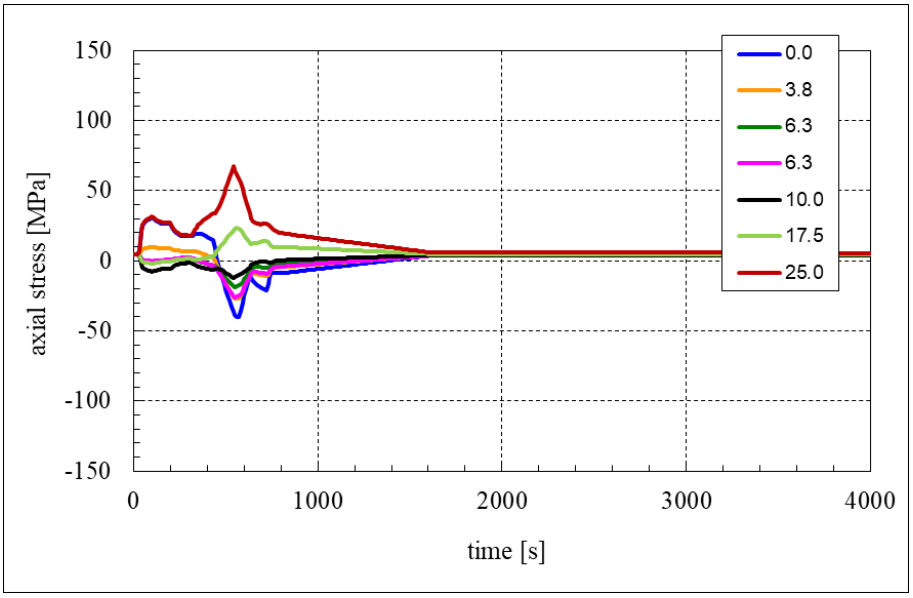

Figure 4-3. ADS transient => Core shroud wall axial stress time history (0 is at inner surface).

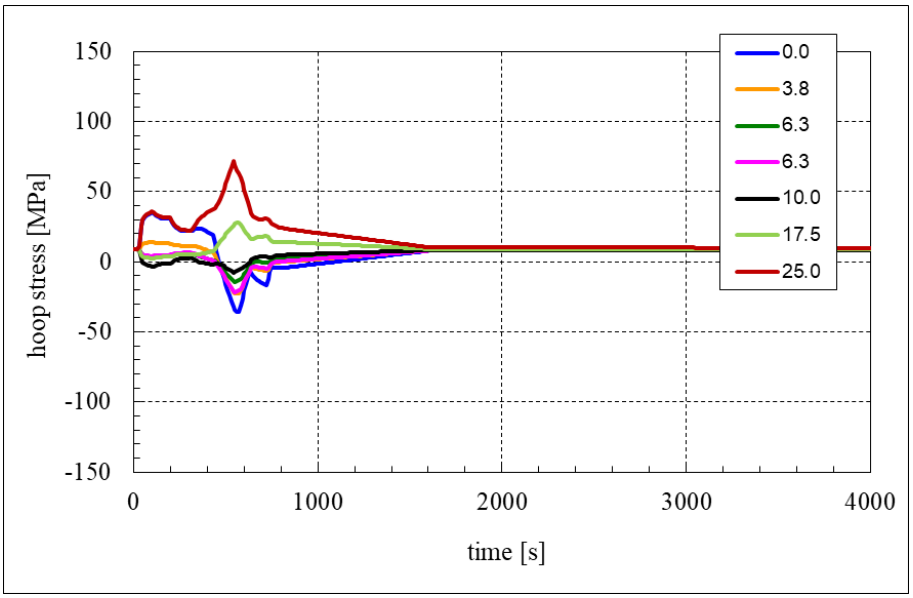

Figure 4-4. ADS transient => Core shroud wall hoop stress time history (0 is at inner surface).

5. Fast fracture analyses

The fast fracture analysis procedure is described in Section 2. The analysis results are presented in the following.

5.1 On the performed analyses

Preliminary analyses for the RPV wall and the core shroud wall showed that even cracks with minimum ligament left will only be critical in case they:

- for circumferential cracks => cover over 180° of the circumference,
- for axial cracks => are several m long.

The aspect ratios of such cracks exceed the scope of the applied K_I solutions. Thus, they are not applicable here. Therefore, K_I solutions for through-wall cracks are used. These are taken from fracture mechanics handbooks [19, 20]. For the considered components the computed stress distributions were used as such in the K_I computations. The applied structural integrity requirement equation is equation (2-2).

5.2 Analysis result summary

The results from the fast fracture analyses are presented in Table 5-1 below. For all reference cracks the maximum K_I value occurs at the crack tip. Therefore K_{Ic} is taken for the temperature at the crack tip. The temperature dependency of K_{Ic} and $K_{I,max}$ values for the RPV wall is illustrated in Figure 5-1. The $K_{I,max}$ values are shown both for axially and circumferentially orientated reference cracks. It has been taken into account that they follow the saturation pressure. As the pressure drops so do the $K_{I,max}$ values. In the legend of Figure 5-1 bm means base material.

Table 5-1. Results from the fast fracture analyses.

Location	Crack	Orientation	Result a x l	K_{Ic} *	$K_{I,max}$	Margin
			[mm]	[MPa√m]	[MPa√m]	[-]
RPV wall	reference	axial	-	240	164	1.46
RPV wall	reference	hoop	-	240	140	1.71
RPV wall	critical	axial	139x813	240	-	-
RPV wall	critical	hoop	139x1635	240	-	-
Core shroud wall	reference	axial	-	350	0	∞
Core shroud wall	reference	hoop	-	350	52	6.73
Core shroud wall	critical	axial	25x1374	350	-	-
Core shroud wall	critical	hoop	25x5648	350	-	-

* The maximum $K_{I,60}$ is applied as K_{Ic} is maximum for T = 60 °C and over, see Figure 5-1. Whenever $K_{I,max}$ has significant values the temperature at the crack tip will be much higher than 60 °C.

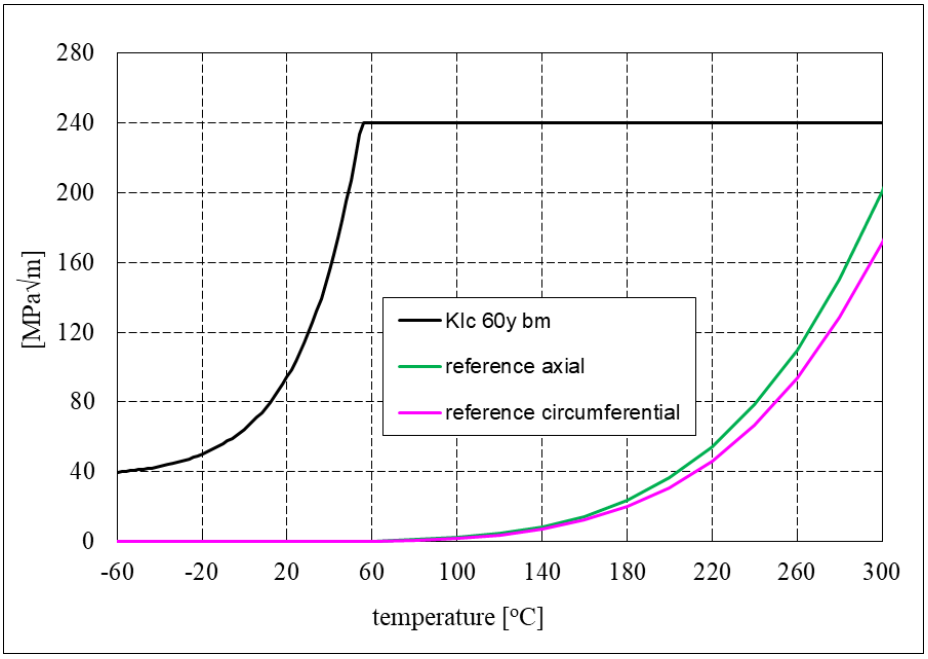

Figure 5-1. The RPV wall => K_{Ic} data and $K_{I,max}$ values for reference cracks under ADS.

6. Summary and conclusions

This study concerns fast fracture analyses to a Finnish BWR RPV and one significant internal component for the most severe anticipated loading event while also taking into account the LTO period. The considered components are the RPV and the core shroud. .

For a list of the locations, types and orientations of the used crack postulates as well as the associated crack sizes from the fast fracture analyses see Table 5-1.

The procedures and criteria of Appendix G of the ASME Section XI [1] are applied. After application of all required safety coefficients the minimum additional margins against fast fracture for the reference cracks is 1.46 for axially orientated reference crack the RPV wall.

The computed sizes of the critical cracks are very large, as follows:

- For the RPV wall, the length of the critical through-wall crack is approximately 800 mm.
- For the core shroud wall, the length of the critical through-wall crack is approximately 5600 mm.

It is concluded that the criteria of ASME Section XI [1] Appendix G are fulfilled. The additional margins against fast fracture are large. It is further concluded that the critical crack sizes are so large that even much smaller cracks would be found during the yearly RPV inspections.

References

1. Section XI, 2017 Edition, ASME Boiler and Pressure Vessel Code, American Society of Mechanical Engineers (ASME).

2. Olkiluoto Nuclear Power Plant Brochure, TVO, TVO Nuclear Power Plant Units 1 and 2.

3. NFPMT DC 70, Rev. D., 2006-11-10, Grandemange, J.M., AREVA NP SIEMENS AG, Report: OL3 Methodology Report on Fast Fracture Prevention According To YVL 3.5 For Pressure Equipment.

4. E 1921-05, 2005, American Society for Testing and Materials (ASTM), ASTM Standard: Standard Test Method for Determination of Reference Temperature, T0, for Ferritic Seels in the Transition Range.

5. VTT-R-00259-17, February 2017, Oinonen, A. and Timperi, A., VTT, Report: VTTBESIM 0.6 User Manual.

6. VTT-R-02089-16, May 2016, Ristaniemi, A., VTT, Report: Programming VTTBESIM with Matlab.

7. EPRI NP-6301-D, June 1989, Zahoor, A., Electric Power Research Institute (EPRI), Report: Ductile Fracture Handbook, Volume 1.

8. Tada, H., Paris, P., Irwin, G., 1985, Paris Productions Incorporated (and Del Research Corporation), Handbook: The Stress Analysis of Cracks, Second Edition.

9. 134814, Rev. C, 13.3.1973, UDDCOMB Sweden AB, Design drawing: TVO I BWR 2000 - Reaktortank.

10. AA 122309, 1973, Asea-Atom, Design Drawing: Moderatortank - System 212.

11. NFPMT DC 70, Rev. D., 2006-11-10, Grandemange, J.M., AREVA NP SIEMENS AG, Report: OL3 Methodology Report on Fast Fracture Prevention According To YVL 3.5 For Pressure Equipment.

12. Section II, 2015 Edition ASME Boiler and Pressure Vessel Code, American Society of Mechanical Engineers (ASME).

13. DMV 347HFG, April 2008, Salzgitter Mannesmann Stainless Tubes GmbH, Material specification: Boiler Grade DMV 347 HFG.

14. SAQ/FoU-Report 96/08, Rev. 3, 1996, Andersson, P., et al., SAQ Kontroll AB, Report: A Procedure for Safety Assessment of Components with Cracks - Handbook.

15. 173415, Version 1, 31.08.2017, Komulainen, E., TVO, Report: OL1 - Reactor Pressure Vessel Nozzle Forces and Moments.

16. PAE 97-349, Rev. 1, 5.11.1997, Götberg, J., ABB Atom AB, Report: OL1 and OL2 - Update of Loading Analyses for the RPV and Internals - ADS Transient Analyses.

17. Raiko, H. et al. Paineistetun termoshokin analysointiohjelma DIFF. Valtion teknillinen tutkimuskeskus (VTT), Valmistustekniikka, työraportti LUJA-1/94. 16.11.1994. 27 p. (in Finnish)

18. SKI Report 2006:23, 2006, Sattari-Far, I., Andersson, M., Statens kärnkraftinspektion (SKI), Cladding Effects on Structural Integrity of Nuclear Components.

19. EPRI NP-6301-D, June 1989, Zahoor, A., Electric Power Research Institute (EPRI), Report: Ductile Fracture Handbook, Volume 1.

20. Tada, H., Paris, P., Irwin, G., 1985, Paris Productions Incorporated (and Del Research Corporation), Handbook: The Stress Analysis of Cracks, Second Edition.